South African Journal of Botany 136 (2021) 81–90

Contents lists available at ScienceDirect

South African Journal of Botany

journal homepage: www.elsevier.com/locate/sajb

QToF exact mass and ESI fragmentation of bioactive Amaryllidaceae alkaloids

L. Torras-Claveria[a,*], S. Berkov[b], F. Viladomat[a], J. Bastida[a]

[a] Grup de Productes Naturals, Departament de Biologia, Sanitat i Medi Ambient, Facultat de Farmàcia i Ciències de l'Alimentació, Universitat de Barcelona, Barcelona, Spain
[b] Institute of Biodiversity and Ecosystem Research, Bulgarian Academy of Sciences, Sofia, Bulgaria

ARTICLE INFO

Article History:
Received 18 February 2020
Revised 16 March 2020
Accepted 22 March 2020
Available online 29 April 2020

Edited by JJ Nair

ABSTRACT

Amaryllidaceae alkaloids are a particular group of alkaloids exclusive to the Amarylloideae subfamily. Important from a biological and pharmacological point of view, they have antiparasitic, antiviral and antitumoral activities. Notably, galanthamine has been approved by the FDA as an acetylcholinesterase inhibitory drug for the treatment of Alzheimer's disease. Overall, Amaryllidaceae alkaloids are easy to analyse by GC–MS, but some are difficult to differentiate or detect. In the current study, some of these problems were resolved by applying an alternative analytical technique, high resolution ESI-MS/MS, a soft ionisation method producing different fragmentation patterns. Amongst the Amaryllidaceae alkaloids, only galanthamine has been previously analysed by high resolution ESI-MS/MS. In this work, a large number of Amaryllidaceae alkaloids were studied by high resolution ESI-MS/MS, providing important new structural information.

1. Introduction

Amaryllidaceae alkaloids are found almost exclusively in plants of the subfamily Amaryllidoideae (of the Amaryllidaceae family). Amaryllidaceae plants have been used for medical purposes throughout history, with references to their usage going back to the Classical period, and today they continue forming part of traditional medicine in many countries. For example, in South Africa, *Ammocharis* is used to treat open wounds, *Brunsvigia* bulbs are applied as an antiseptic, and *Clivia* species serve to treat snakebites and facilitate birth. In Asia and South America, *Crinum* species are used to treat tumours, haemorrhoids and gynaecological conditions, and to clean wounds (Torras-Claveria et al., 2017). Amaryllidaceae alkaloids have a wide range of biological and pharmacological activities, which are the basis of many of these traditional medicinal applications. Amongst their proven properties are antiparasitic, antiviral, antitumoral and acetylcholinesterase-inhibitory activities. The alkaloid galanthamine, a potent acetylcholinesterase inhibitor, is currently commercialised for the palliative treatment of mild to moderate Alzheimer's disease (Bastida et al., 2011). Narciclasine-type alkaloids such as pancratistatine and narciclasine are attracting considerable attention because of their specific anticancer activities with minimal effects on normal cells (Nair et al., 2012).

According to Ghosal's model, Amaryllidaceae alkaloids can be classified into 9 skeleton types formed from the common precursor *O*-methylnorbelladine. However, it has recently been proposed that the 636 structures of isolated or tentatively identified alkaloids can be classified more accurately into 42 skeleton types (Berkov et al., 2020). Notably, recently reported dinitrogenous plicamine-type alkaloids with 2 nitrogens have been proposed as new members of this group (de Andrade et al., 2012).

Several selective apoptosis-inducing effects have been associated with different structural types of Amaryllidaceae alkaloids, and structure-activity relationship studies (SAR) have been performed (Mc Nulty et al., 2009a, 2009b; Nair et al., 2012). In this context, there is a demand for potent and selective methods to analyse these alkaloids.

Amaryllidacae alkaloids have been successfully analysed by HPLC-MS and GC–MS. Capillary-electrophoresis-MS also constitutes a promising strategy (Zang and Chen, 2013; El Deeb et al., 2016), although its relatively low sensitivity has precluded a widespread application and in the pharmaceutical area it is regarded as a complimentary tool (Suntorsuk, 2007).

GC–MS has become one of the most popular methods for identifying Amaryllidaceae alkaloids owing to its ability to rapidly recognise specific compounds in a plant extract or isolated pure compounds without a derivatisation step. It is also highly sensitive and allows a correct volatilisation of this kind of alkaloids in gas chromatographic conditions (Smith, 2004; Berkov et al., 2008; Torras-Claveria et al., 2010, 2011). The ionisation method used is electron

* Corresponding author.
E-mail address: lauratorras@hotmail.com (L. Torras-Claveria).

https://doi.org/10.1016/j.sajb.2020.03.024
0254-6299/

Table 1
Lycorine-type alkaloid fragmentation and exact mass obtained with ESI-MS/MS-Q-ToF (CE=25).

Alkaloid	$[M+H]^+$	Calculated $[M+H]^+$	ESI Fragments (%)
Lycorine	288.1228	288.1236	119.0472 (30), **147.0428 (100)**, 177.0535 (20), 194.0955 (10), 222.0902 (10), 252.1002 (10), 270.1109 (20), 288.1218 (20)
Pseudolycorine	290.1376	290.1392	119.0472 (30), **147.0432 (100)**, 179.0685 (20), 194.0945 (10), 222.0897 (10), 240.0997 (10), 257.1028 (10), 272.1267 (20), 290.1369 (30)
Incartine	334.1622	334.1654	**191.0684 (100)**, 199.0962 (70), 214.0846 (70), 272.1259 (50)
2-*O*-hydroxybutyryllycorine	372.1433	374.1604	250.0847 (20), 269.0986 (20), 268.0958 (100), **272.1438 (100)**
Kirkine	272.1270	274.1443	201.0882 (20), 215.0994 (20), 228.1008 (70), 244.1285 (25), 256.1304 (20), **272.1269 (100), 290.1371 (20)**
Hippadine	264.0648	264.0661	178.0639 (60), **206.0592 (100)**, 234.0540 (30), 264.0646 (20)
8-*O*-demethylvasconine	252.1022	253.1103	180.8000 (10), **209.0836 (100)**, 210.0863 (20), 237.0781 (50), 252.1020 (20)
Oxoassoanine	282.1118	282.1130	191.0718 (10), 209.0825 (10), 220.0755 (20), 237.0773 (10), 238.0858 (50), **266.0812 (100)**, 282.1121 (20)
Ungeremine	266.0828	266.0817	151.0531 (20), 152.0609 (50), 180.0796 (30), 191.0718 (20), 207.0675 (50), **208.0751 (100)**, 236.0698 (10), 266.0809 (20)
1-Acetyllycorine	330.1345	330.1341	82.0631 (70), **134.0591 (100)**, 147.0433 (90), 194.0956 (60), 222.0911 (50), 270.1121 (40), 230.1332 (10)
Epilycorine	288.1237	288.1236	91.0527 (20), 119.0481 (45), **147.0432 (100)**, 177.0550 (10), 194.0956 (20), 222.0907 (20), 270.1121 (20), 288.1221 (30)
Sternbergine	332.1499	332.1498	82.0628 (30), **134.0588 (100)**, 147.0426 (40), 179.0690 (20), 194.0950 (20), 222.0908 (50), 229.1054 (30), 240.1000 (20), 254.1159 (20), 257.1038 (40), 272.1261 (40), 332.1472 (30)
Galanthine	318.1701	318.1705	147.0427 (20), **162.0662 (100)**, 165.0895 (20), 193.0848 (40), 237.1129 (30), 254.1154 (20), 268.1318 (20), 271.1192 (30), 286.1427 (30), 318.1684 (20)

impact (EI), which provides an extensive fragmentation of the molecule upon submission to a beam of highly energetic electrons, usually with an energy of 70 eV. However, this system is not suitable for all alkaloids; for example, *N*-oxide forms are unstable under GC conditions and some molecular EI ionised ions have low stability, such as those from homolycorine-type alkaloids (de Andrade et al., 2016).

Electrospray ionisation (ESI) is a softer technique, resulting in minimal fragmentation, which can facilitate the detection and determination of the exact mass of ions not found in an EI spectrum. Specifically, it converts the HPLC or CE containing the sample effluent into an aerosol, which is subjected to a high voltage. Furthermore, when the ESI source is coupled to MS/MS, the energy applied for the molecular fragmentation can be controlled, so no ions are missed. However, EI and ESI fragments can show slight variations and the molecule can follow different fragmentation pathways (Smith, 2004).

LC-MS/MS with ESI has been successfully employed to analyse galanthamine from rat, mouse and rabbit plasma (Geerts et al., 2005), beagle dog plasma (Jahn et al., 2012), human plasma (Zhao et al., 2005; Nirogi et al., 2007; Noetzli et al., 2012) and rat blood (Goh et al., 2011). LC-MS/MS has also proved to be a useful tool for analysing complex mixtures of alkaloids such as in plant extracts, allowing Zhang et al. (2009) to determine crinane- and tazettine type alkaloids in the species *Crinum latifolium* and *Crinum asiaticum*. However, no ESI database has been developed for Amaryllidaceae alkaloids, and only a few of which have ESI data in the literature.

In this study, several Amaryllidaceae alkaloids, previously studied in our group by GC–MS and identified by spectroscopic techniques such as NMR, CD and IR, were analysed using ESI ionisation and high resolution MS/MS and detected by ToF. To our knowledge, this is the first time that a large collection of Amaryllidaceae alkaloids has been analysed by ESI-Q-ToF and the resulting exact mass and ESI fragmentation data are presented. Furthermore, EI and ESI-MS/MS fragmentation pathways for lycorine, haemanthamine, galanthamine, and homolycorine are compared.

2. Experimental

2.1. Pure compounds

The pure Amaryllidaceae alkaloids used were previously isolated from a large variety of Amaryllidaceae plants and identified by GC–MS, NMR and other spectroscopic techniques such as IR and CD in our laboratory. They were prepared at 10–25 μg/mL in MeOH and directly injected into an LC-MS/MS apparatus.

2.2. LC-ESI-TOF-MS/MS analysis

The LC system was an Agilent 1200 binary pump (Waldbronn, Germany) with an autosampler and a thermostatically controlled column compartment. The LC column was a Luna C_{18} (150×2.1 mm, 5 μm particle size) (Phenomenex, Torrance, CA, USA). A gradient elution was applied with 0.05% aqueous CH_3COOH (v/v) (solvent A) and MeOH (solvent B). The gradient was the following (min,%B): (0, 5), (15, 100), (25, 100), (25.5, 5) and (30, 5). The flow rate was constant at 400 μL/min and the injection volume 15 μL.

The LC system was coupled to a mass spectrometer (QSTAR Elite hybrid Quadrupole-Time of Flight (QToF) (Applied Biosystems, PE Sciex, Concord, Ontario, Canada). Data were recorded from *m/z* 70 to 700 with an accumulation time of 1 s and a pause between the mass range of 0.55 ms, operating in the positive mode. The Q1 transmission window was 50.1% for *m/z* 80 and 49.9% for *m/z* 190. The instrument parameter settings were the following: capillary voltage 4000 V, nebuliser gas (N_2) 40 (arbitrary units), curtain gas (N_2) 50 (arbitrary units), collision gas (N_2) 5 (arbitrary units), focusing potential 380 V, declustering potentials (DP) 80 V and (DP2) 10 V, and

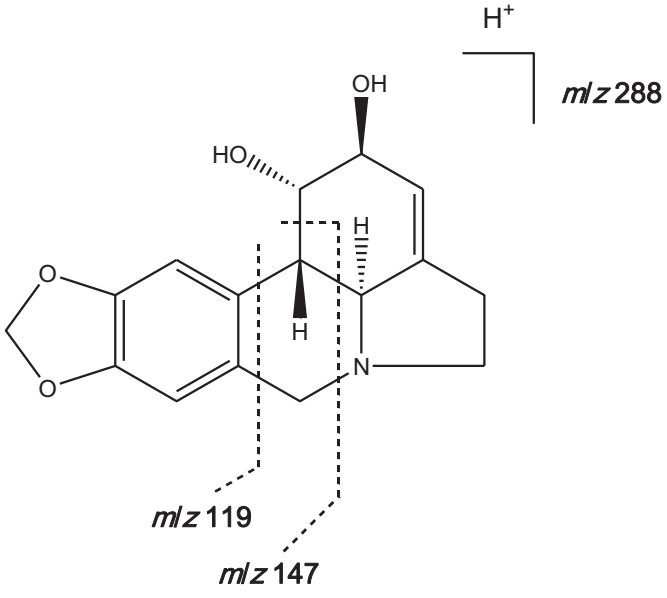

Fig. 1. Possible ESI fragmentation of lycorine according to Zhou et al. (2014).

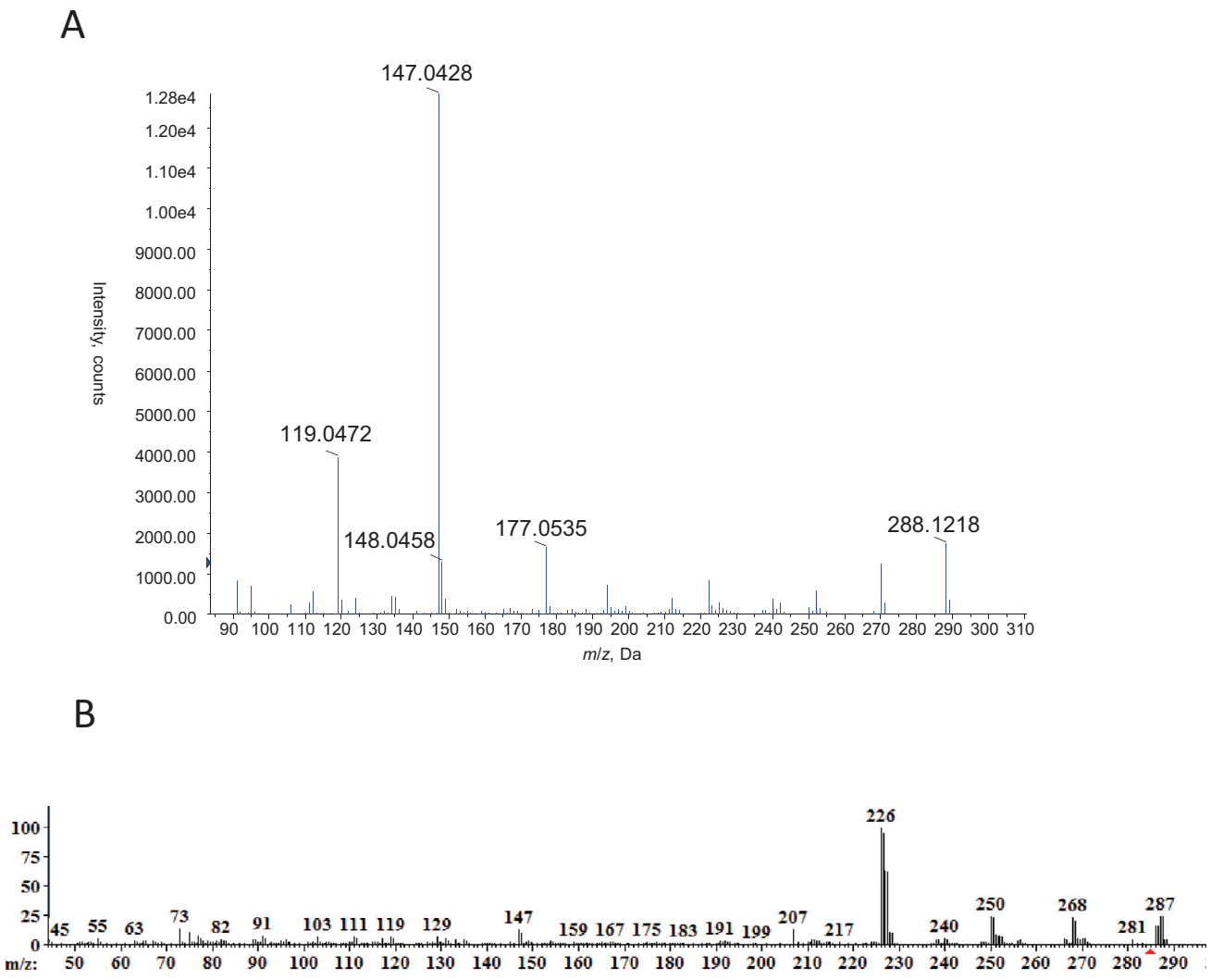

Fig. 2. Comparative fragmentation of lycorine by ESI (A) and EI-GC–MS (B).

drying gas (N_2) 70 (arbitrary units) heated to 400°C. Collision energy (CE) varied from 20 to 40 (arbitrary units). Acquisition and data analyses were performed by Analyst QS version 2.0 software (Applied Biosystems, PE Sciex, Concord, Ontario, Canada).

2.3. GC–MS analysis

GC–MS analyses were performed in an Agilent 6890 N coupled to an MSD GC5975 (Agilent Technologies, Santa Clara, CA, USA), operating in EI mode at 70 eV. An HP-5 MS column (30 m x 0.25 mm i.d. x 0.25 μm film thickness) (Agilent Technologies, Santa Clara, CA, USA) was used. The temperature gradient performed was the following: 100–180° C at 15 °C/min, 1 min hold at 180 °C and 180–300° C at 5 ° C / min, and hold at 300° C for 40 min. The injector temperature was at 280 °C and the flow rate of carrier gas (helium) 0.8 mL/min. The split ratio was 1:5. RI values of compounds were measured with a standard *n*-hydrocarbon calibration mixture (C9-C36) using AMDIS 2.64 software.

3. Results and discussion

High resolution exact mass and ESI-MS/MS fragments of 59 alkaloids of lycorine (**13**)-, homolycorine (**8**)-, galanthamine (**10**)-, crinane (**19**)-, and tazettine (**3**)-types together with 3 dinitrogenous alkaloids were determined using LC-ESI-MS/MS.

Reported here for the first time is the exact mass of 13 lycorine-type alkaloids (lycorine, pseudolycorine, incartine, 2-*O*-hydroxybutirryllycorine, kirkine, hippadine, 8-*O*-demethylvasconine, oxoassoanine, ungeremine, 1-*O*-acetyllycorine, epilycorine, sternbergine, and galanthine), 8 galanthamine-type alkaloids (chlidanthine, narwedine, lycoramine, lycoraminone, sanguinine, acetylsanguinine, habranthine, and *N*-formylnorgalanthamine) and epimacronine. Also reported for the first time is the ESI-MS/MS fragmentation for 8 galanthamine-type alkaloids (epigalanthamine, epinorgalanthamine, chlidanthine, lycoraminone, acetylsanguinine, habranthine, sanguinine, and *N*-formylnorgalanthamine), 8 homolycorine-type alkaloids (candimine, hippeastrine, lycorenine, homolycorine, 8-*O*-demethylhomolycorine, 6-*O*-methyllycorenine, clivonine and clivimine), tazettine, pretazettine and epimacronine. Other alkaloids analysed show an exact mass and ESI-MS/MS fragmentation in agreement with the literature (Mroczek et al., 2009; Zhang et al., 2009; Katoch et al., 2012; de Andrade et al., 2012; Zhang and Chen, 2013; Bessa et al., 2017).

3.1. Lycorine type

The ESI-MS/MS fragmentation and exact mass of 13 lycorine-type alkaloids were determined, as summarised in Table 1. Lycorine shows an exact mass of *m/z* 288.1228 corresponding to the $[M + H]^+$ ion, and *m/z* 147.0428 as the main fragment. This ion is also present in GC–MS

Table 2
Crinane-type alkaloid fragmentation and exact mass obtained with ESI-MS/MS-Q-ToF.

Alkaloid	$[M+H]^+$	Calculated $[M+H]^+$	ESI Fragments (%)
Haemanthamine type			
Haemanthamine	302.1368	302.1392	CE=40 153.0678 (60), 168.0786 (40), 181.0632 (70), **196.0741 (100)**, 211.0729 (35), 226.0846 (40), 270.1104 (20), 302.1365 (15)
Crinamine	302.1371	302.1392	CE=40 153.0674 (80), 168.0777 (40), **181.0624 (100)**, 196.0728 (70), 211.0699 (50), **224.0683 (90), 226.0837 (90)**, 270.1102 (20), 302.1361 (15)
6-Hydroxycrinamine	318.1323	318.1341	CE=30 169.0628 (20), 197.0581 (40), **199.0736 (100)**, 211.0728 (40), **227.0682 (55)**, 268.0950 (40), 318.1321 (30)
Haemanthidine	318.1311	318.1341	CE=30 169.0624 (30), 197.0576 (50), **199.0727 (80)**, 209.0574 (60), 211.0726 (50), **225.0860 (50), 227.0676 (100)**, 268.0948 (60), 286.1057 (40), 318.1319 (60)
Vitattine	272.1262	272.1287	CE=40 108.0784 (20), 134.0574 (20), 136.0728 (50), 167.0743 (20), 168.0778 (50), 196.0731 (100), 224.0824 (20), 226.0828 (45), 254.1138 (20), 272.1248 (50)
11-Hydroxyvitattine	288.1193	288.1236	CE=40 152.0588 (30), **153.0669 (60)**, 168.0777 (50), **181.0618 (65), 196.0727 (100)**, 201.0810 (30), 211.0712 (35), **226.0830 (50)**, 227.0886 (30), 288.1193 (30)
Papyramine	318.1695	318.1705	CE=30 215.1056 (60), 229.1218 (80), 245.1042 (50), 257.1166 (70), 268.1329 (60), **286.1435 (100)**, 318.1701 (40)
Hamayne	288.1219	288.1236	CE=40 152.0595 (40), **153.0675 (90)**, 155.0829 (30), 168.0782 (60), 173.0573 (30), **181.0626 (100)**, 183.0777 (30), **196.0733 (90)**, 211.0709 (50), **224.0686 (75), 226.0841 (80)**, 227.0891 (35), 288.1215 (30)
11-*O*-Hydroxybutanoylhamayne	374.1601	374.1604	CE=40 149.0589 (30), 194.0959 (40), 222.0908 (60), 250.0865 (30), **252.1018 (100)**, 374.1592 (20)
3,11-Dihydroxybutanoylhamayne	460.1960	460.1971	CE=35 222.0909 (30), **252.1022 (100)**, 460.1960 (70)
3,3′-Dihydroxybutanoylhamayne	460.1951	460.1971	CE=35 165.0684 (20), 181.0638 (50), 193.0640 (40), 211.0740 (30), 223.0742 (60), 226.0842 (20), **252.1007 (100), 270.1112 (100)**, 356.1478 (20), 442.1830 (20), 460.1942 (20)
11,3′-Dihydroxybutanoylhamayne	460.1956	460.1971	CE=35 223.0737 (20), **252.1013 (100)**, 270.1114 (50), 356.1478 (40), 460.1946 (40)
Narcidine	304.1531	304.1549	CE=35 153.0686 (30), 168.0793 (30), 181.0637 (80), 183.0784 (20), **196.0746 (100)**, 213.0891 (70), 215.1050 (25), 228.1006 (60), 272.1271 (30), 304.1531 (50)
Crinine type			
Crinine	272.1265	272.1287	CE=40 108.0782 (30), 134.0571 (20), 136.0727 (50), 167.0745 (20), 168.0778 (50), 196.0730 (100), 224.0706 (20), 226.0830 (50), 254.1134 (20), 272.1247 (50)
Elwesine	274.1448	274.1443	CE=50 118.0642 (40), **120.0798 (100)**, 198.0908 (40), 226.0856 (30), 228.1014 (60), 256.1330 (50), 274.1432 (40)
Ambeline	332.1483	332.1498	CE=40 153.0684 (45), 165.0607 (70), 183.0770 (80), 185.0937 (45), **211.0731 (100)**, 213.0889 (70), 226.0835 (50), 243.0965 (55), 271.0957 (70), 282.1116 (50), 332.1490 (30)
11-Acetylambeline	374.1586	374.1604	CE=35 106.0639 (10), 130.0643 (10), 165.0543 (30), 224.1053 (30), 252.1002 (30), 267.0880 (20), **282.1111 (100)**, 374.1585 (30)
6-Hydroxybuphanidrine	332.1500	332.1498	CE=35 203.0692 (30), 229.0845 (50), **243.1006 (100)**, 259.0827 (40), 282.1111 (40), 300.1228 (40), 332.1492 (10)
6-Ethoxybuphanidrine	360.1808	360.1811	CE=30 224.1054 (20), 252.1007 (40), 254.0809 (30), **282.1112 (100)**, 314.1372 (20), 360.1803 (10)

fragmentation but at a much lower intensity and could correspond to the left part of the molecule, as shown in Fig. 1 (Zhou et al., 2014). The second most intense fragment for lycorine is at *m/z* 119, corresponding to the aromatic and dimethoxy part. This suggests that soft ionisation tends to fragment the molecule differently compared to a high intensity method such as EI. The main ions in ESI fragmentation are 119, 147, 177 and 288, and in EI fragmentation 147 (with a very low intensity), 226, 250, 268 and 287. In Fig. 2, which compares lycorine fragmentation by EI-GC–MS and ESI, it can be seen that although some fragments are common to both techniques, their intensity differs considerably. The ESI fragmentation of lycorine is in agreement with previous studies (Katoch et al., 2012; Zhang and Chen, 2013; Zhou et al., 2014; Tian et al., 2015).

Incartine shows a base ion of *m/z* 191.0684, corresponding to rings A and B. Therefore, its fragmentation is different from lycorine because the base ion includes the whole B ring.

On the other hand, 2-*O*-hydroxybutyryllycorine, kirkine and 8-*O*-demethylvasconine have an $[M+H]^+$ ion with one or two hydrogens less than the calculated $[M+H]^+$ ion, suggesting some molecule degradation prior to ESI.

3.2. Crinane type

Crinane-type alkaloids have a characteristic ethano bridge at the α or β position, giving rise to conformers like vittatine (α position) and crinine (β position) that cannot be distinguished by techniques such as GC–MS.

The exact mass and ESI fragmentation of 19 crinane-type Amaryllidaceae alkaloids are summarised in Table 2.

Haemanthamine shows an $[M+H]^+$ ion at *m/z* 302.1268 and a characteristic fragment of *m/z* 270 corresponding to the loss of the substituent in C3. Also, fragments at *m/z* 211 and 181 agree with the proposed fragmentation of its isomer crinamine (Zhang et al., 2009; Katoch et al., 2012). Crinamine, a conformer of haemanthamine, has the methoxyl substituent at the α position of C3, unlike in haemanthamine, where it is at the β position. Although the two alkaloids share a common $[M+H]^+$ ion at *m/z* 302.1392, they differ significantly in ESI mass spectra, as shown in Fig. 3. Whereas both share ions at *m/z* 270, 226, 211, 196, 181, 168 and 153, the relative intensities are very different. Haemanthamine has a dominant ion at *m/z* 196, and crinamine at *m/z* 181; also, in haemanthamine the ion at *m/z* 226 is far less intense than in crinamine. These differences allow the two alkaloids to be differentiated, which is not possible with GC–MS analysis.

The fragmentation pattern of the different crinane-type alkaloids differs considerably from that obtained by GC–MS. For example, the ion at *m/z* 226, corresponding to the loss of *N*-methylforminine via a retro Diels-Alder (RDA) process, is common in haemanthamine, crinamine, vitattine, crinine, 11-hydroxyvitattine, hamayne, elwesine, ambeline and 3,3′-dihydroxybutanoylhamayne when analysed by ESI but absent with EI GC–MS. Fig. 4 compares the ESI and EI fragmentation of haemanthamine and depicts the structure of the most important ions.

3.3. Galanthamine type

Galanthamine, owing to its use as a commercial drug for the treatment of Alzheimer's disease, is one of the most analysed Amaryllidaceae alkaloids, both in plant extracts and body fluids. Several studies

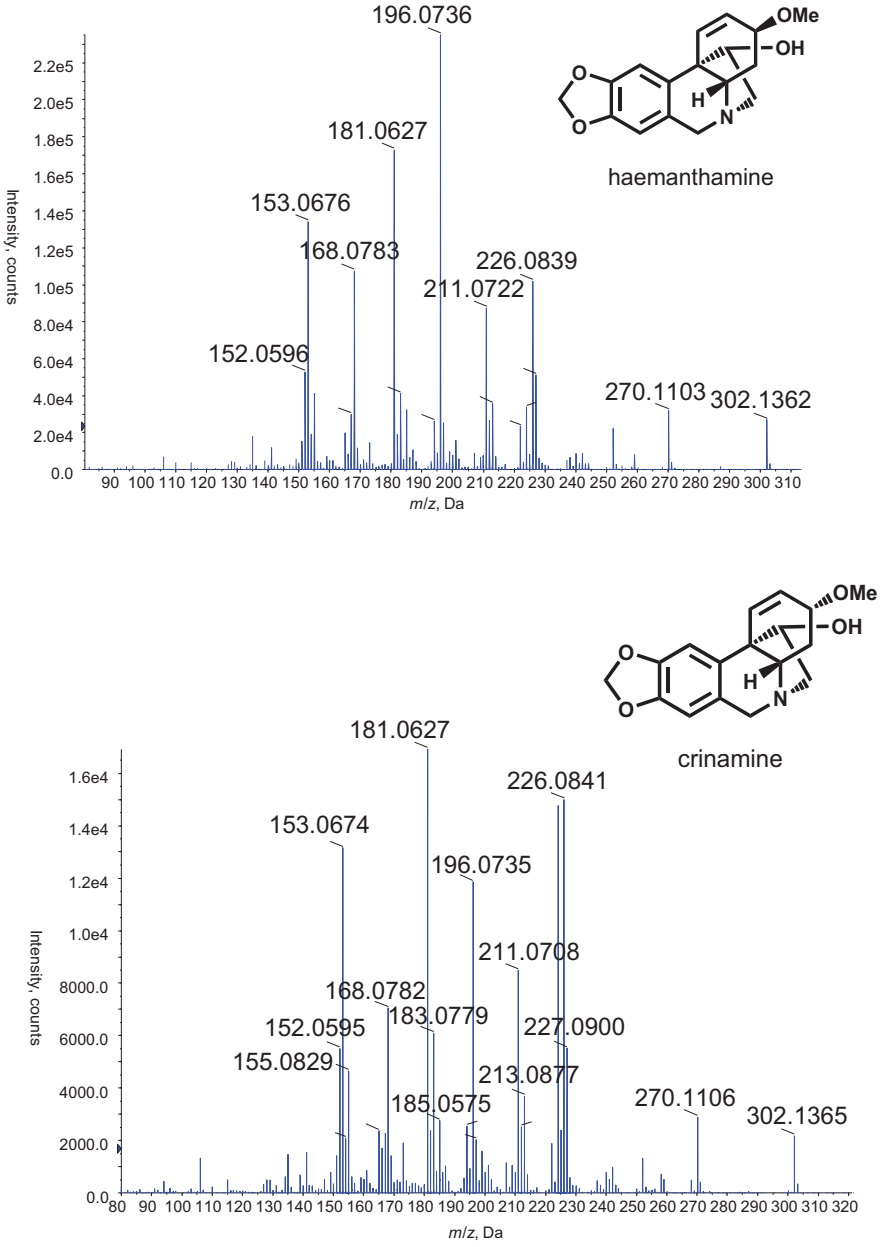

Fig. 3. Different ESI fragmentation pattern for haemanthamine and crinamine.

have used LC-MS to detect galanthamine (Verhaeghe et al., 2003; Thevis et al., 2006; Nirogi et al., 2007; Mess et al., 2009; Mzroczek et al., 2009; Park et al., 2012; Steiner et al., 2012; Cuthbertson et al., 2013; Zhou et al., 2014; Saliba et al., 2016). The ESI fragmentation and exact mass obtained for galanthamine in the current work are in agreement with the literature (Thevis et al., 2006; Cuthbertson et al., 2013; Zhou et al., 2014; Tian et al., 2015), with the dominant fragment at *m/z* 213 and minor fragments at *m/z* 198, 225, 231, and 270. However, scarce ESI ionisation and fragmentation data are available for other galanthamine-type alkaloids (Tian et al., 2015). Here, 9 galanthamine-type alkaloids were analysed for the first time, and the high resolution exact mass and ESI fragmentation data of 10 galanthamine-type alkaloids are provided in Table 3. The mass spectra of epigalanthamine and galanthamine are very similar and difficult to differentiate, although they can be distinguished by GC–MS (Berkov et al., 2008). The characteristic galanthamine fragment of *m/z* 213 was also obtained in epinorgalanthamine, lycoraminone, sanguinine, acetylsanguinine, habranthine, and *N*-formylnorgalanthamine by ESI fragmentation. This fragment was first proposed to arise from methylvinylamine and water (Verhaeghe et al., 2003). However, a new pathway leading to the fragment *m/z* 213 was subsequently described, suggesting a different structure (Thevis et al., 2006). Our analysis of sanguinine is in agreement with this new route, because the structure of the *m/z* 213 fragment has a hydroxyl at position 9 instead of the methoxy group of galanthamine and other galanthamine-type alkaloids. Thus, another possible structure of the *m/z* 213 fragment ion is proposed (Fig. 5), following the route suggested by Thevis et al. (2006).

As in lycorine- and crinane-type alkaloids, ESI and EI-GC–MS fragmentation patterns were completely different. For example, for galanthamine (Fig. 6), although the ion at *m/z* 270 is obtained with both techniques, the main fragments by GC–MS are at *m/z* 286, 244, 216 and 174, in comparison with *m/z* 288, 270, 231, 225, 213 and 198 in ESI fragmentation.

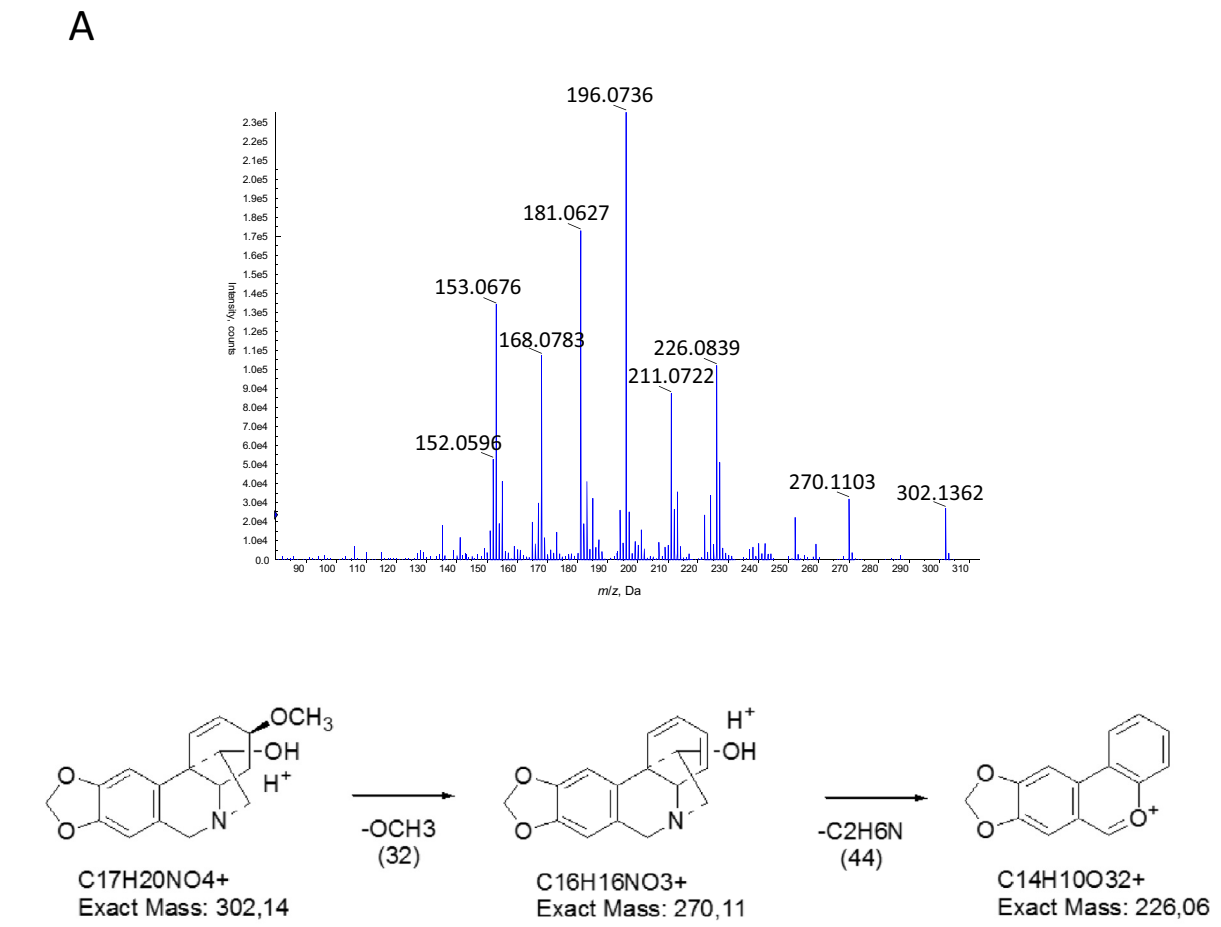

Fig. 4. ESI fragmentation of haemanthamine with the fragmentation pathway and struture of most important ions (A) and comparison with its EI fragmentation from GC–MS (B).

Table 3
Galanthamine-type alkaloid fragmentation and exact mass obtained with ESI-MS/MS-Q-ToF.

Alkaloid	$[M+H]^+$	Calculated $[M+H]^+$	ESI Fragments (%)
Galanthamine	288.1590	288.1600	CE=30 198.0665 (30), **213.0908 (100)**, 225.0901 (20), 231.1008 (30), 270.1485 (10), 288.1580 (10)
Epigalanthamine	288.1588	288.1600	CE=30 181.1008 (10), 198.0672 (30), 209.0962 (30), **213.0916 (100)**, 270.1489 (10), 288.1593 (10)
Epinorgalanthamine	274.1455	274.1443	CE=30 182.0723 (10), 198.0669 (30), **213.0908 (100)**, 231.1016 (20), 274.1456 (10)
Chlidanthine	288.1590	288.1600	CE=30 184.0514 (10), **199.0813 (100)**, 231.1014 (10), 239.1068 (10), 256.1331 (5), 288.1595 (5)
Narwedine	286.1446	286.1443	CE=35 141.0695 (10), 158.0727 (40), 173.0957 (20), 179.0851 (20), 182.0722 (15), 186.0668 (10), 197.0957 (40), **201.0915 (100)**, 210.0674 (10), 214.0623 (10), 225.0917 (50), **229.0867 (90)**, 286.1440 (10)
Lycoraminone	288.1604	288.1600	CE=35 161.0948 (60), 175.0754 (40), 203.1054 (80), 213.0889 (20), **231.1023 (100)**, 288.1601 (20)
Acetylsanguinine	316.1546	316.1549	CE=30 184.0523 (20), **199.0788 (100)**, 209.0961 (20), 225.0919 (20), 256.1355 (40), 316.1554 (10)
Habranthine	304.1550	304.1549	CE=30 198.0676 (20), **213.0981 (100)**, 231.1017 (20), 304.1553 (20)
Sanguinine	274.1453	274.1443	CE=30 182.0735 (10), 198.0682 (30), **213.0920 (100)**, 231.1028 (20), 274.1460 (10)
N-Formylnorgalanthamine	302.1392	302.1392	CE=30 198.0662 (30), 211.0742 (30), **213.0904 (100)**, 225.0899 (35), 239. 1054 (30), 302.1374 (20)

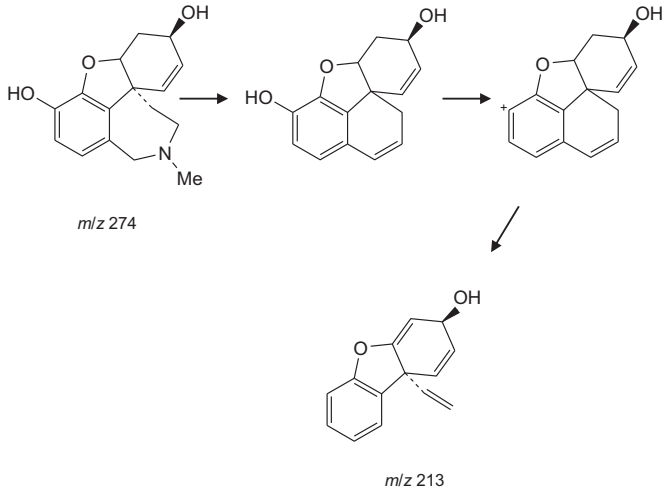

Fig. 5. Alternative fragmentation route leading to *m/z* 213 for sanguinine based on Thevis et al. (2006).

3.4. Homolycorine type

EI fragmentation of homolycorine-type alkaloids is characterised by a prominent *m/z* 109 ion corresponding to the pyrrolidine ring. The very low intensity of all other fragments, however, can make it difficult to differentiate these compounds by GC–MS. In contrast, as ESI fragmentation can be modulated in terms of CE and DP, these alkaloids present more variation: for example, the *m/z* 109 ion is completely absent in all compounds fragmentation while the fragment *m/z* 191 is common to candimine, hippeastrine, lycorenine and 6-*O*-methyllycorenine (Table 4). On the other hand, homolycorine shows a fragment ion at *m/z* 300, corresponding to the loss of the methyl group of the nitrogen (Fig. 7). There are few references to LC-MS analysis of homolycorine-type Amaryllidaceae alkaloids (Bessa et al., 2017), and to our knowledge this is the first report of their ESI fragmentation.

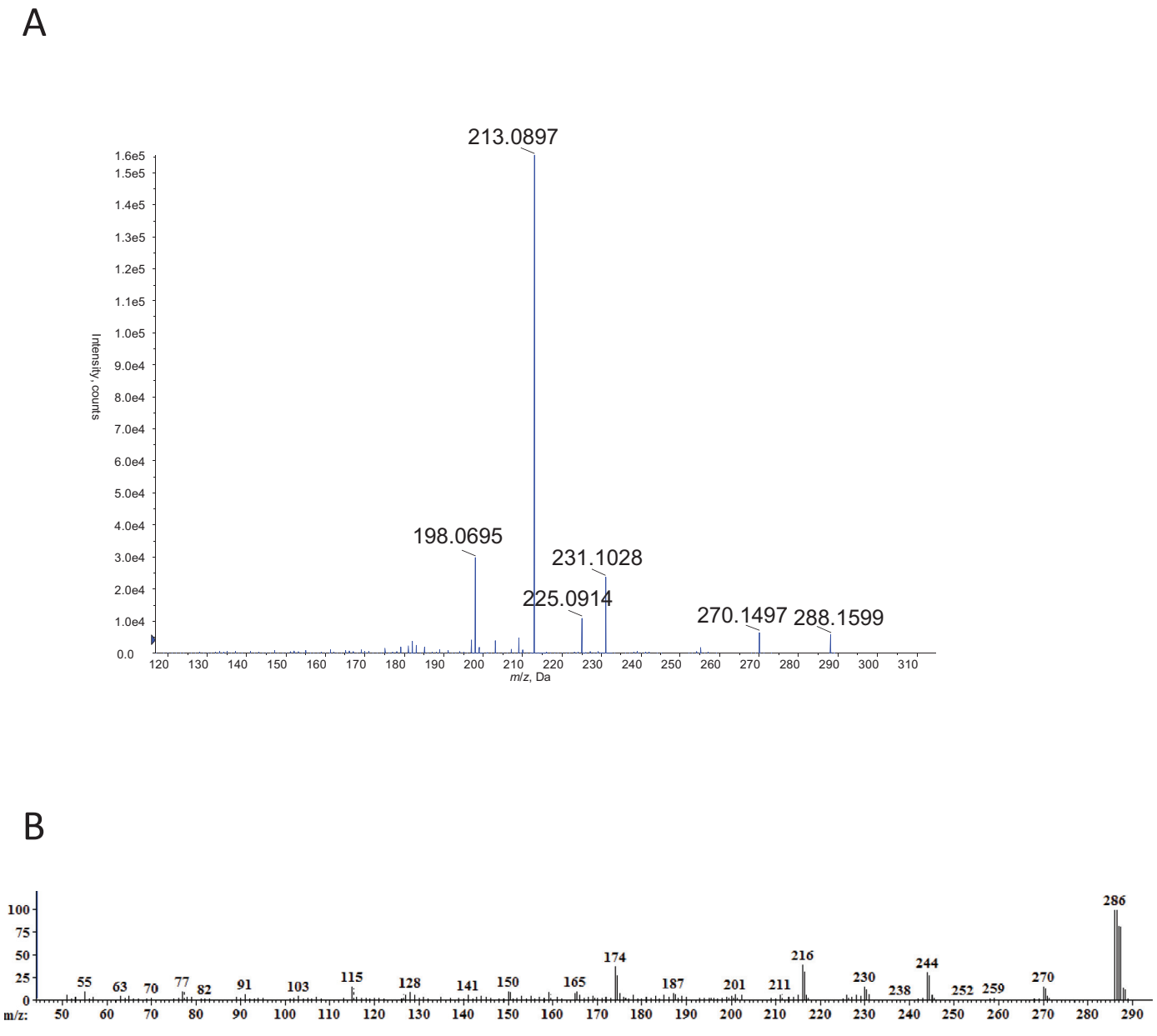

Fig. 6. Comparative fragmentation of galanthamine by ESI (A) and EI-GC–MS.

Table 4
Homolycorine-type alkaloid fragmentation and exact mass obtained with ESI-MS/MS-Q-ToF.

Alkaloid	$[M+H]^+$	Calculated $[M+H]^+$	ESI fragments (%)
Candimine	346.1296	346.1291	CE=40 **221.0446 (100), 205.0497** (30), **346.1294** (30), 96.0798 (25), 163.0388 (25), 177.0546 (20), 191.0336 (25), 257.0819 (25), 269.0824 (25), 292.0970 (20), 295.0841 (20), 328.1184 (20)
Hippeastrine	316.1188	316.1185	CE=40 147.0434 (20), **153.0688** (55), 165.0690 (25), 169.0638 (20), 175.0382 (40), **181,0639 (100), 191.0333** (50), 194.0952 (25), 197.0589 (20), 209.0591 (30), 222.0902 (40), 227.0697 (25), **239.0698** (50), 252.1000 (20), **262.0854** (40), 265,0720 (20), 273.0978 (25), 280.0961 (25), 298.1070 (25), **316.1176** (40)
Lycorenine	318.1726	318.1705	CE=35 151.0740 (25), 165.0680 (20), 181.0677 (20), **191.0698 (100)**, 195.0784 (30), 207.0797 (25), 210.1026 (40), 214.0981 (25), 225.0898 (25), 226.0977 (40), 229.1214 (50), 238.0987 (30), **239.1058** (70), **251.1164** (60), **257.1172** (50), 269.1181 (25), 284.1276 (30), **300.1590 (100)**, 318.1695 (30)
Homolycorine	316.1548	316.1549	CE=40 189.0854 (30), 195.0651 (40), 207.0603 (30), 236.1000 (60), 239.1191 (25), 254.1060 (25), **265.1021** (70), 267.1128 (30), **282.1050** (50), **300.1156 (100)**, 316.1463 (30)
8-*O*-Demethylhomolycorine	302.1400	302.1392	CE=45 115.0531 (20), 153.0684 (20), 165.0678 (20), 181.0581 (25), 214.1215 (20), 223.0974 (25), 242.1164 (20), **251.0935 (100)**, 252.0995 (30), 269.1039 (35), 284.1277 (25), 287.1148 (30), 302.1386 (20)
6-*O*-methyllycorenine	332.1770	332.1862	CE=30 191.0649 (50), 251.1224 (20), 257.1105 (20), **300.1519 (100)**, 332.1768 (30)
Clivonine	318.1352	318.1341	CE=40 **96.0794 (100)**, 165.0693 (20), 175.0382 (20), 193.0655 (20), 225.0536 (20), 239.0708 (50), 241.0741 (80), 251.0703 (30), 254.0973 (20), 267.0898 (25), 272.1010 (20), 282.1116 (20), 285.0988 (80), 300.1234 (80), 318.1352 (30)
Clivimine	794.2964	794.2925	CE=35 162.0545 (30), 251.0700 (20), 282.1129 (20), **300.1236 (100)**, 477.1669 (60), 794.2935 (20)

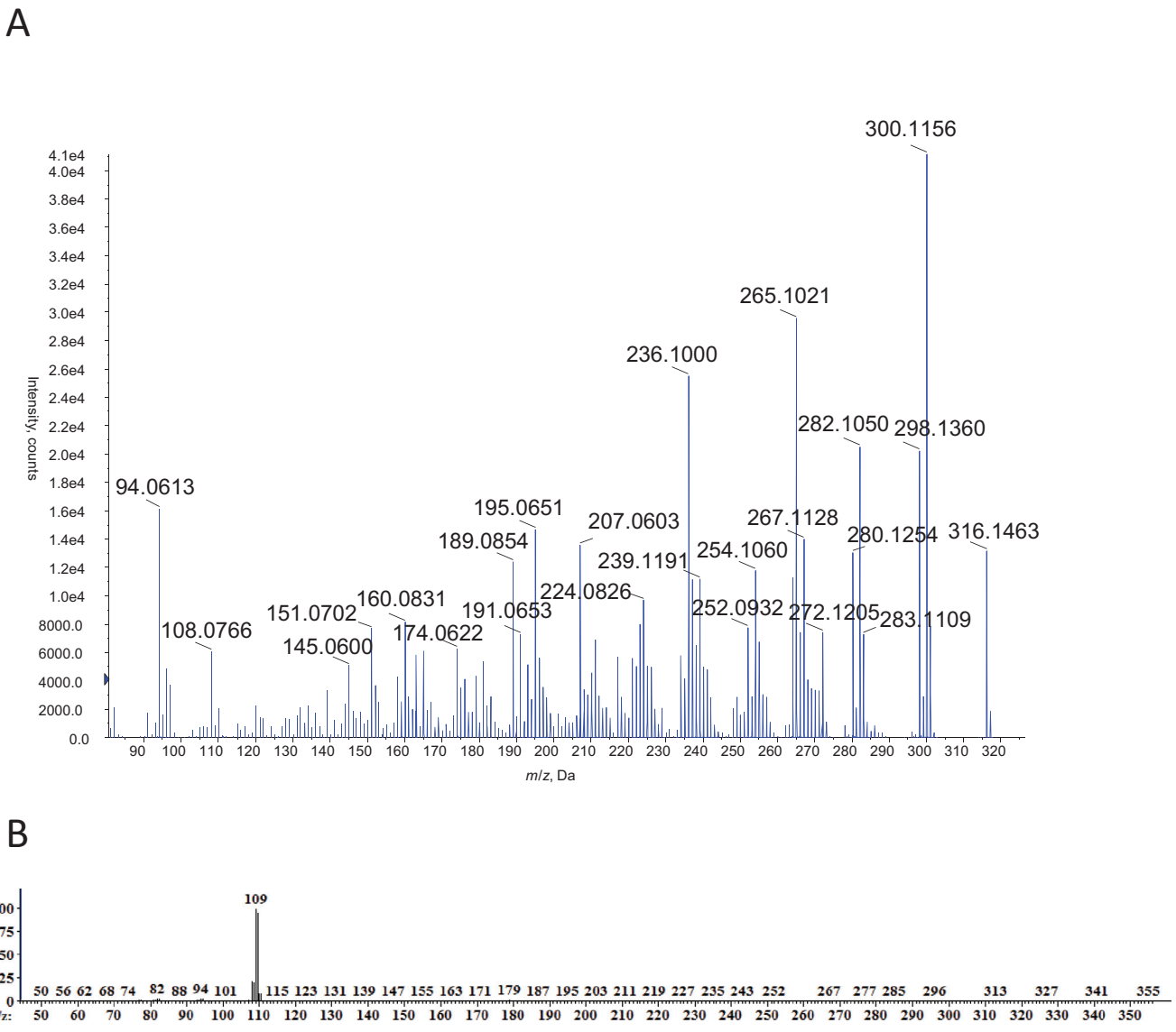

Fig. 7. Comparative fragmentation of homolycorine by ESI (A) and EI-GC–MS.

Table 5
Plicamine-type alkaloid-fragmentation and exact mass obtained with ESI-MS/MS-Q-ToF.

Alkaloid	$[M+H]^+$	Calculated $[M+H]^+$	ESI fragments (%)
Obliquine	449.2070	449.2081	CE=40 121.0666 (60), 244.1021 (50), 269.1337 (20), **329.1585 (100)**, 364.1625 (20), 449.2176 (10)
Plicamine	463.1873	463.1874	CE=40 **121.0659 (100)**, 226.0538 (20), 258.0804 (20), 343.1365 (90), 369.1515 (10), 463.1964 (10)
Secoplicamine	465.2047	465.2031	CE=30 121.0653 (10), 181.0674 (20), 211.0790 (20), **348.1313 (100)**, 374.1457 (10), 465.2024 (10)

3.5. Dinitrogenous type

ESI ionisation was especially useful for this particular group of alkaloids, resulting in the fragmentation pattern depicted in Table 5, as they show no fragmentation pattern when analysed by EI-GC–MS. They have a common fragment ion of *m/z* 121, which corresponds to 4-hydroxyphenethyl. This ion is particularly intense in plicamine, indicating that it corresponds to an early fragmentation. The fragmentation observed for these unusual compounds is in agreement with that reported by de Andrade et al. (2012).

3.6. Tazettine type

Tazettine has proved to be an artefact arising from pretazettine during the alkaloid acid-base extraction procedure from plants (de Andrade et al., 2012), and the naturally present metabolite is pretazettine. Pretazettine is also converted to tazettine during GC–MS analysis, which gives an identical fragmentation pattern and retention index for both. Pretazettine can only be detected by CG-MS after derivatisation with BSTFA, when the introduced substituent blocks the conversion reaction to tazettine.

In contrast, tazettine can be easily distinguished from pretazettine by ESI-MS/MS analysis, as they show different fragmentation patterns (Table 6). In tazettine the base fragment is the ion at *m/z* 314, obtained via a retro Diels Alder reaction as depicted in Fig. 8, whereas in pretazettine it is the $[M+H]^+$ ion at *m/z* 332.

Other tazettine-type alkaloids such as latifaliumins have been analysed by ESI-MS/MS (Zhang et al., 2009), but to our knowledge this is the first report of ESI-MS/MS fragmentation and high resolution MS analysis of tazettine, pretazettine and epimacronine.

Table 6
Tazettine-type alkaloid fragmentation and exact mass obtained with ESI-MS/MS-Q-ToF.

Alkaloid	$[M+H]^+$	Calculated $[M+H]^+$	ESI fragments (%)
Tazettine	332.1480	332.1498	CE=25 181.0624 (20), 211.0741 (10), 282.1097 (10), **314.1389 (100)**, 332.1501 (10)
Pretazettine	332.1485	332.1498	CE=25 225.0893 (20), 300.1212 (30), 314.1357 (40), **332.1466 (100)**
Epimacronine	330.1338	330.1341	CE=35 171.0804 (20), 199.0745 (20), 225.0546 (20), 227.0699 (40), **239.0686 (100)**, 255.0647 (40), 255.0647 (40), 272.0919 (40), 330.1344 (30)

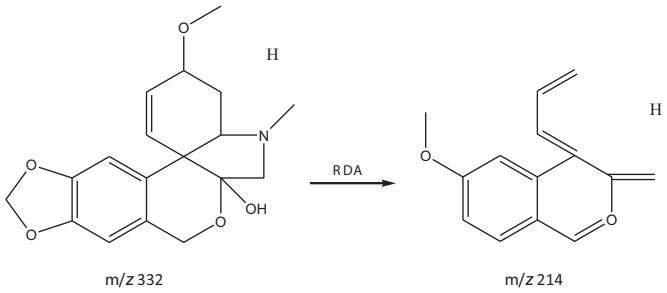

Fig. 8. Structure of the main tazettine fragment after Retro Diels Alder fragmentation by ESI .

4. Conclusions

ESI and EI fragmentation differed considerably in all the Amaryllidaceae alkaloid types analysed. LC-ESI-MS/MS fragmentation and exact mass yielded valuable information for the identification of Amaryllidaceae alkaloids that in GC–MS analysis undergo excessive fragmentation, such as homolycorine-type alkaloids, or are undetectable, such as dinitrogenous-type alkaloids. The technique used in the current work was also able to identify pretazettine, which in GC–MS analysis is converted to tazettine. To the best of our knowledge, this is the first time a large collection of isolated Amaryllidaceae alkaloids has been analysed by ESI-MS/MS, resulting in a valuable exact mass and ESI fragmentation database that will be useful for future studies of medicinal plants.

Declaration of Competing Interest

The authors declare that they have no known competing financial interests or personal relationships that could have appeared to influence the work reported in this paper.

Aknowledgements

L.T-C. and J.B. are members of the Research Group 2017-SGR-604 at the University of Barcelona.

References

Bastida, J., Berkov, S., Torras, L., Pigni, N.B., de Andrade, J.P., Martínez, V., Codina, C., Viladomat, F., 2011. Chemical and biological aspects of amaryllidaceae alkaloids. In: Muñoz-Torrero, D. (Ed.), Recent Advances in Pharmaceutical Sciences. Transword Research Network, Kerala, pp. 65–100.

Berkov, S., Bastida, J., Viladomat, F., Codina, C., 2008. Analysis of galanthamine-type alkaloids by capillary gas chromatography-mass spectrometry in plants. Phytochemical Analysis 19, 285–293.

Berkov, S., Bastida, J., Viladomat, F., Codina, C., 2011. Development and validation of a gc-ms method for a rapid determination of galanthamine in *leucojum aestivum* and *narcissus* ssp.: a metabolomic approach. Talanta 83, 1455–1465.

Berkov, S., Osorio, E., Viladomat, F., Bastida, J., 2020. Chemodiversity, chemotaxonomy and chemoecology of amaryllidaceae alkaloids. In: Knolker, H.J. (Ed.), The Alkaloids. 83, Elsevier Inc, Amsterdam.

Bessa, C.D.P.B., de Andrade, J.P., de Oliveira, R.S., Domingos, E., Santos, H., Romão, W., Bastida, J., Borges, W.S., 2017. Identification of alkaloids from *hippeastrum aulicum* (Ker gawl.) herb. (Amaryllidaceae) using cgc-ms and ambient ionization mass spectromentry (PS-MS and LS-MS). Journal of the Brazilian Chemical Society 28, 819–830.

Cuthbertson, D.J., Johnson, S.R., Piljac-Žegarac, J., Kappel, J., Schäfer, S., Wüst, M., Ketchum, R.E.B., Croteau, R.B., Marques, J.V., Davin, L.B., Lewis, N.G., Rolf, M., Kutchan, T.M., Soejarto, D.D., Lange, B.M., 2013. Accurate mass-time tag library for LC/MS-based metabolite profiling of medicinal plants. Phytochemistry 91, 187–197.

de Andrade, J.P., Pigni, N.B., Torras-Claveria, L., Berkov, S., Codina, C., Viladomat, F., Bastida, J., 2012. Bioactive alkaloid extracts from *narcissus broussonetii*: mass spectral studies. Journal of Pharmaceutical and Biomedical Analysis 70, 13–25.

de Andrade, J.P., Giordani, R.B., Torras-Claveria, L., Pigni, N.B., Berkov, S., Font-Bardia, M., Calvet, T., Konrath, E., Bueno, K., Sachett, L.G., Dutilh, J.H.,

Borges, W.S., Viladomat, F., Henriques, A.T., Nair, J.J., Zuanazzi, J.A.S., Bastida, J., 2016. The Brazillian amaryllidaceae as a source of acetylcholinesterase inhibitory alkaloids. Phytochemistry Reviews 15, 147–160.
El Deeb, S., Wätzig, H., El-Hady, D.A., Sänger-van de Griend, C., Scriba, G.K.E., 2016. Recent advances in capillary eletrophoretic migration techniques for pharmaceutical analysis (2013-2015). Electrophoresis 37, 1591–1608.
Geerts, H., Guillaumat, P., Grantham, C., Bode, W., Anciaux, K., Sachak, S., 2005. Brain levels and acetylcholinesterase inhibition with galanthamine and donepezil in rats, mice, and rabbits. Brain Research 1033, 186–193.
Goh, C.W., Aw, C.C., Lee, J.H., Chen, C.P., Browne, E.R., 2011. Pharmacokinetic and pharmacodynamic properties of cholinesterase inhibitors donepezil, tacrine, and galantamine in aged and young lister hooded rats. Drug Metabolism & Disposition 39, 402–411.
Jahn, S., Seiwert, B., Kretzing, S., Abraham, G., Regenthal, R., Karst, U., 2012. Metabolic studies of the *amaryllidaceous* alkaloids galanthamine and lycorine based on electrochemical simulation in addition to *in vivo* and *in vitro* models. Analytica Chimica Acta 756, 60–72.
Katoch, D., Kumar, S., Kumar, N., Singh, B., 2012. Simultaneous quantification of amaryllidaceae alkaloids from *zephyranthes grandiflora* by uplc-dad/esi-ms/ms. Journal of Pharmaceutical and Biomedical Analysis 71, 187–192.
Mc Nulty, J., Nair, J.J., Bastida, J., Pandey, S., Griffin, C., 2009a. Structure activity studies on the crinane alkaloid apoptosis-inducing pharmacophore. Natural Product Communications 4, 483–488.
Mc Nulty, J., Nair, J.J., Bastida, J., Pandey, S., Griffin, C., 2009b. Structure-activity studies on the lycorine pharmacophore: a potent inducer of apoptosis in human leukemia cells. Phytochemistry 70, 913–919.
Mess, J.N., Lahaie, M., Furtado, M., Garofolo, F., 2009. Effect of high pH mobile phase on the sensitivity of multiple drugs by lc positive electrospray ionization ms/ms. Bioanalysis 1, 1419–1430.
Mroczek, T., 2009. Highly efficient, selective and sensitive molecular screening of acetylcholinesterase inhibitors of natural origin by solid-phase extraction-liquid chromatography/electrospray ionisation-octopole-orthogonal acceleration time-of-flight-mass spectrometry and novel thin-layer chromatography-based bioautography. Journal of Chromatography A 1216, 2519–2528.
Nair, J.J., Bastida, J., Viladomat, F., van Staden, J., 2012. Cytotoxic agents of the crinane series of amaryllidaceae alkaloids. Natural Product Communications 7, 1677–1688.
Nirogi, R.V., Kandikere, V.N., Mudigonda, K., Maurya, S., 2007. Quantitative determination of galantamine in human plasma by sensitive liquid chromatography-tandem mass spectrometry using loratadine as internal standard. Journal of Chromatographic Science 45, 97–103.
Noetzli, M., Ansermot, N., Dobrinas, M., Eap, C.B., 2012. Simultaneous determination and antidementia drugs in human plasma: procedure transfer from hplc-ms to uplc-ms/ms. Journal of Pharmaceutical and Biomedical Analysis 64-65, 16–25.
Park, Y.S., Kim, S.H., Kim, S.Y., Kim, Y.H., Lee, M.H., Yang, S.C., Shaw, L.M., Kang, J.S., 2012. Quantification of galantamine in human plasma by validated liquid chromatography-tandem mass spectrometry using glimepride as an internal standard: application to bioavailability studies in 32 healthy korean subjects. Journal of Chromatographic Science 50, 803–809.
Saliba, S., Ptak, A., Boisbrun, M., Spina, R., Dupire, F., Laurain-Mattar, D., 2016. Stimulating effect of both 4'- *O* -methylnorbelladine feeding and temporary immersion conditions on galanthamine and lycorine production by *leucojum aestivum* L. bulblets. Engineering in Life Sciences 16, 731–739.
Smith, R.M., 2004. Understanding Mass Spectra. A Basic Approach, second ed. J. Wiley &; Sons, New Jersey.
Steiner, W.E., Pikalov, I.A., Williams, P.T., English, W.A., Hilmas, C.J., 2012. Development of a Novel LC/MS/MS Extraction Assay for Galanthamine in Guinea Pig Plasma and its Application to Nerve Agent Countermeasures. OMICS International. Open Access Scientific Reports 1: Report 149.
Suntornsuk, L., 2007. Capillary electrophoresis in pharmaceutical analysis: a survey on recent applications. Journal of Chromatographic Science 45, 559–577.
Thevis, M., Wilkens, F., Geyer, H., Schänzer, W., 2006. Determination of therapeutics with growth-hormone secretagogue activity in human urine for doping control purposes. Rapid Communications in Mass Spectrometry 20, 3393–3402.
Tian, Y., Zhang, C., Guo, M., 2015. Comparative analysis of amaryllidaceae alkaloids from three *lycoris* species. Molecules 20, 21854–21869.
Torras-Claveria, L., Berkov, S., Jáuregui, O., Caujapé, J., Viladomat, F., Codina, C., Bastida, J., 2010. Metabolic profiling of bioactive *pancratium canariense* extracts by gc-ms. Phytochemical Analysis 21, 80–88.
Torras-Claveria, L., Tallini, L., Viladomat, F., Bastida, J., 2017. Research in natural products: amaryllidaceae ornamental plants as sources of bioactive compounds. In: Muñoz-Torrero, D., Feliu, C. (Eds.), Recent Advances in Pharmaceutical Sciences. Transworld Research Network, Trivandrum. Kerala, India, pp. 69–82.
Verhaeghe, T., Diels, L., de Vries, R., de Meulder, M., de Jong, J., 2003. Development and validation of a liquid chromatographic-tandem mass spectrometric method for the determination of galantamine in human heparinised plasma. Journal of Chromatography B 789, 337–346.
Zhang, X., Huang, H., Liang, X., Huang, H., Dai, W., Shen, Y., Yan, S., Zhang, W., 2009. Analysis of amaryllidaceae alkaloids from *crinum* by high-performance liquid chromatography coupled with electrospray ionization tandem mass spectrometry. Rapid Communications in Mass Spectrometry 23, 2903–2916.
Zhang, Y., Chen, Z., 2013. Nonaqueous ce esi-it-ms analysis of amaryllidaceae alkaloids. Journal of Separation Science 36, 1078–1084.
Zhao, Q., Janssens, L., Verhaeghe, T., Brashear, H.R., Truyen, L., 2005. Pharmacokinetics of extended-release and immediate-release formulations of galanthamine at steady state in healthy volunteers. Current Medical Research and Opinion 21, 1547–1554.
Zhou, X., Liu, Y., Huang, S., Liu, Y., 2014. An lc-ms/ms method for the simultaneous determination of lycorine and galanthamine in rat plasma and its application to pharmacokinetic study of *lycoris radiata* extract in rats. Journal of Huazhong University of Science and Technology 34, 861–868.